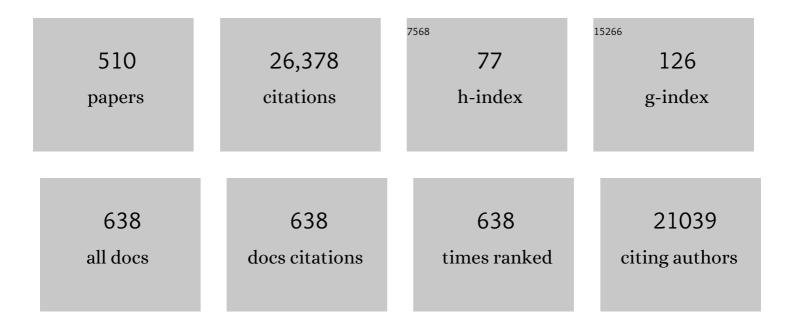
Jianmin Chen

List of Publications by Year in descending order

Source: https://exaly.com/author-pdf/411254/publications.pdf Version: 2024-02-01



#	Article	IF	CITATIONS
1	Investigating aldehyde and ketone compounds produced from indoor cooking emissions and assessing their health risk to human beings. Journal of Environmental Sciences, 2023, 127, 389-398.	6.1	14
2	A critical review of sulfate aerosol formation mechanisms during winter polluted periods. Journal of Environmental Sciences, 2023, 123, 387-399.	6.1	20
3	Sources of variation in simulated ecosystem carbon storage capacity from the 5th Climate Model Intercomparison Project (CMIP5). Tellus, Series B: Chemical and Physical Meteorology, 2022, 66, 22568.	1.6	17
4	Application of smog chambers in atmospheric process studies. National Science Review, 2022, 9, nwab103.	9.5	21
5	<i>p</i> -Phenylenediamine Antioxidants in PM _{2.5} : The Underestimated Urban Air Pollutants. Environmental Science & Technology, 2022, 56, 6914-6921.	10.0	61
6	Atmospheric gaseous organic acids in winter in a rural site of the North China Plain. Journal of Environmental Sciences, 2022, 113, 190-203.	6.1	5
7	Mechanistic toxicity assessment of fine particulate matter emitted from fuel combustion via pathway-based approaches in human cells. Science of the Total Environment, 2022, 806, 150214.	8.0	4
8	Source apportionment of PM2.5 during haze episodes in Shanghai by the PMF model with PAHs. Journal of Cleaner Production, 2022, 330, 129850.	9.3	30
9	An online technology for effectively monitoring inorganic condensable particulate matter emitted from industrial plants. Journal of Hazardous Materials, 2022, 428, 128221.	12.4	9
10	Toxic potency-adjusted control of air pollution for solid fuel combustion. Nature Energy, 2022, 7, 194-202.	39.5	59
11	Absorption Enhancement of Black Carbon Aerosols Constrained by Mixing-State Heterogeneity. Environmental Science & Technology, 2022, 56, 1586-1593.	10.0	18
12	Connecting the Oxidative Potential of Fractionated Particulate Matter With Chromophoric Substances. Journal of Geophysical Research D: Atmospheres, 2022, 127, .	3.3	5
13	Existence and Formation Pathways of High- and Low-Maturity Elemental Carbon from Solid Fuel Combustion by a Time-Resolved Study. Environmental Science & Technology, 2022, 56, 2551-2561.	10.0	15
14	Significant impactor sampling artifacts of ammonium, nitrate, and organic acids. Atmospheric Environment, 2022, 274, 118985.	4.1	2
15	Regional Transport of PM _{2.5} and O ₃ Based on Complex Network Method and Chemical Transport Model in the Yangtze River Delta, China. Journal of Geophysical Research D: Atmospheres, 2022, 127, .	3.3	5
16	Photodissociation of particulate nitrate as a source of daytime tropospheric Cl2. Nature Communications, 2022, 13, 939.	12.8	26
17	Characterization of peroxyacetyl nitrate (PAN) under different PM2.5 concentration in wintertime at a North China rural site. Journal of Environmental Sciences, 2022, 114, 221-232.	6.1	5
18	More Than Concentration Reduction: Contributions of Oxidation Technologies to Alleviating Aerosol Toxicity from Diesel Engines. Environmental Science and Technology Letters, 2022, 9, 280-285.	8.7	5

#	Article	IF	CITATIONS
19	Atmospheric measurements at Mt. Tai – Part I: HONO formation and its role in the oxidizing capacity of the upper boundary layer. Atmospheric Chemistry and Physics, 2022, 22, 3149-3167.	4.9	12
20	Characteristics of aerosol chemistry and acidity in Shanghai after PM2.5 satisfied national guideline: Insight into future emission control. Science of the Total Environment, 2022, 827, 154319.	8.0	13
21	pH modifies the oxidative potential and peroxide content of biomass burning HULIS under dark aging. Science of the Total Environment, 2022, 834, 155365.	8.0	13
22	Accurate observation of black and brown carbon in atmospheric fine particles via a versatile aerosol concentration enrichment system (VACES). Science of the Total Environment, 2022, 837, 155817.	8.0	4
23	Formation of Secondary Nitroaromatic Compounds in Polluted Urban Environments. Journal of Geophysical Research D: Atmospheres, 2022, 127, .	3.3	11
24	Molecular characterization of nitrogen-containing organic compounds in the winter North China Plain. Science of the Total Environment, 2022, 838, 156189.	8.0	5
25	Constraining Microplastic Particle Emission Flux from the Ocean. Environmental Science and Technology Letters, 2022, 9, 513-519.	8.7	13
26	Field Detection of Highly Oxygenated Organic Molecules in Shanghai by Chemical Ionization–Orbitrap. Environmental Science & Technology, 2022, 56, 7608-7617.	10.0	11
27	Liquid-liquid phase separation reduces radiative absorption by aged black carbon aerosols. Communications Earth & Environment, 2022, 3, .	6.8	16
28	Real-time single particle characterization of oxidized organic aerosols in the East China Sea. Npj Climate and Atmospheric Science, 2022, 5, .	6.8	4
29	Polycyclic aromatic hydrocarbons (PAHs) in gas, PM2.5, and frost samples in a severely polluted rural site of the North China Plain: Distribution, source, and risk assessment. Science of the Total Environment, 2022, 844, 156919.	8.0	11
30	Characterizing Atmospheric Brown Carbon and Its Emission Sources during Wintertime in Shanghai, China. Atmosphere, 2022, 13, 991.	2.3	7
31	Spatiotemporal variation, source and secondary transformation potential of volatile organic compounds (VOCs) during the winter days in Shanghai, China. Atmospheric Environment, 2022, 286, 119203.	4.1	11
32	Nano-Al2O3 particles affect gut microbiome and resistome in an in vitro simulator of the human colon microbial ecosystem. Journal of Hazardous Materials, 2022, 439, 129513.	12.4	4
33	Metals, PAHs and oxidative potential of size-segregated particulate matter and inhalational carcinogenic risk of cooking at a typical university canteen in Shanghai, China. Atmospheric Environment, 2022, 287, 119250.	4.1	4
34	Size distributions of particle-generated hydroxyl radical (·OH) in surrogate lung fluid (SLF) solution and their potential sources. Environmental Pollution, 2021, 268, 115582.	7.5	11
35	On-site analysis of COVID-19 on the surfaces in wards. Science of the Total Environment, 2021, 753, 141758.	8.0	16
36	Diverse bacterial populations of PM2.5 in urban and suburb Shanghai, China. Frontiers of Environmental Science and Engineering, 2021, 15, 1.	6.0	12

#	Article	IF	CITATIONS
37	Nitrous acid emission from open burning of major crop residues in mainland China. Atmospheric Environment, 2021, 244, 117950.	4.1	11
38	Increased new particle yields with largely decreased probability of survival to CCN size at the summit of Mt. Tai under reduced SO ₂ emissions. Atmospheric Chemistry and Physics, 2021, 21, 1305-1323.	4.9	8
39	Fuel Aromaticity Promotes Low-Temperature Nucleation Processes of Elemental Carbon from Biomass and Coal Combustion. Environmental Science & amp; Technology, 2021, 55, 2532-2540.	10.0	17
40	A semicontinuous study on the ecotoxicity of atmospheric particles using a versatile aerosol concentration enrichment system (VACES): development and field characterization. Atmospheric Measurement Techniques, 2021, 14, 1037-1045.	3.1	5
41	Direct Observation of Sulfate Explosive Growth in Wet Plumes Emitted From Typical Coalâ€Fired Stationary Sources. Geophysical Research Letters, 2021, 48, e2020GL092071.	4.0	17
42	Magnetic Particles Unintentionally Emitted from Anthropogenic Sources: Iron and Steel Plants. Environmental Science and Technology Letters, 2021, 8, 295-300.	8.7	15
43	Chemical Fingerprinting of HULIS in Particulate Matters Emitted from Residential Coal and Biomass Combustion. Environmental Science & amp; Technology, 2021, 55, 3593-3603.	10.0	41
44	Intermediate Volatile Organic Compound Emissions from Residential Solid Fuel Combustion Based on Field Measurements in Rural China. Environmental Science & Technology, 2021, 55, 5689-5700.	10.0	39
45	Characterizing Black Carbon and Gaseous Pollutants on the Yangtze River Across Eastern China Continent. Journal of Geophysical Research D: Atmospheres, 2021, 126, e2020JD033488.	3.3	1
46	Iceâ€Nucleating Particle Concentrations and Sources in Rainwater Over the Third Pole, Tibetan Plateau. Journal of Geophysical Research D: Atmospheres, 2021, 126, e2020JD033864.	3.3	0
47	Spatially explicit analysis identifies significant potential for bioenergy with carbon capture and storage in China. Nature Communications, 2021, 12, 3159.	12.8	58
48	Molecular composition and optical property of humic-like substances (HULIS) in winter-time PM2.5 in the rural area of North China Plain. Atmospheric Environment, 2021, 252, 118316.	4.1	18
49	Particle-Phase Photoreactions of HULIS and TMIs Establish a Strong Source of H ₂ O ₂ and Particulate Sulfate in the Winter North China Plain. Environmental Science & Technology, 2021, 55, 7818-7830.	10.0	24
50	Extreme Exposure Levels of PCDD/Fs Inhaled from Biomass Burning Activity for Cooking in Typical Rural Households. Environmental Science & Technology, 2021, 55, 7299-7306.	10.0	14
51	Performance comparison of SMPSs with soft X-ray and Kr-85 neutralizers in a humid atmosphere. Journal of Aerosol Science, 2021, 154, 105756.	3.8	3
52	Modeled changes in source contributions of particulate matter during the COVID-19 pandemic in the Yangtze River Delta, China. Atmospheric Chemistry and Physics, 2021, 21, 7343-7355.	4.9	23
53	Toxicity Assessment of Nano-ZnO Exposure on the Human Intestinal Microbiome, Metabolic Functions, and Resistome Using an In Vitro Colon Simulator. Environmental Science & Technology, 2021, 55, 6884-6896.	10.0	24
54	Substantial changes in gaseous pollutants and chemical compositions in fine particles in the North China Plain during the COVID-19 lockdown period: anthropogenic vs. meteorological influences. Atmospheric Chemistry and Physics, 2021, 21, 8677-8692.	4.9	22

#	Article	IF	CITATIONS
55	High Pressure Inside Nanometer-Sized Particles Influences the Rate and Products of Chemical Reactions. Environmental Science & Technology, 2021, 55, 7786-7793.	10.0	12
56	Atmospheric Nitrate Formation through Oxidation by Carbonate Radical. ACS Earth and Space Chemistry, 2021, 5, 1801-1811.	2.7	5
57	Characterization of a Kanomax® fast condensation particle counter in the sub-10 nm range. Journal of Aerosol Science, 2021, 155, 105772.	3.8	8
58	PM _{1.0} -Nitrite Heterogeneous Formation Demonstrated via a Modified Versatile Aerosol Concentration Enrichment System Coupled with Ion Chromatography. Environmental Science & Technology, 2021, 55, 9794-9804.	10.0	6
59	Association of PM _{2.5} with Insulin Resistance Signaling Pathways on a Microfluidic Liver–Kidney Microphysiological System (LK-MPS) Device. Analytical Chemistry, 2021, 93, 9835-9844.	6.5	5
60	Predicting the effect of confinement on the COVID-19 spread using machine learning enriched with satellite air pollution observations. Proceedings of the National Academy of Sciences of the United States of America, 2021, 118, .	7.1	16
61	Atmospheric Hydrogen Peroxide (H 2 O 2) at the Foot and Summit of Mt. Tai: Variations, Sources and Sinks, and Implications for Ozone Formation Chemistry. Journal of Geophysical Research D: Atmospheres, 2021, 126, e2020JD033975.	3.3	7
62	Measurement report: Biogenic volatile organic compound emission profiles of rapeseed leaf litter and its secondary organic aerosol formation potential. Atmospheric Chemistry and Physics, 2021, 21, 12613-12629.	4.9	4
63	Commodity plastic burning as a source of inhaled toxic aerosols. Journal of Hazardous Materials, 2021, 416, 125820.	12.4	39
64	Measurement report: Saccharide composition in atmospheric fine particulate matter during spring at the remote sites of southwest China and estimates of source contributions. Atmospheric Chemistry and Physics, 2021, 21, 12227-12241.	4.9	7
65	Halogens Enhance Haze Pollution in China. Environmental Science & Technology, 2021, 55, 13625-13637.	10.0	22
66	The roles of aqueous-phase chemistry and photochemical oxidation in oxygenated organic aerosols formation. Atmospheric Environment, 2021, 266, 118738.	4.1	14
67	Fine particle pH and its influencing factors during summer at Mt. Tai: Comparison between mountain and urban sites. Atmospheric Environment, 2021, 261, 118607.	4.1	7
68	Compositions, sources, and potential health risks of volatile organic compounds in the heavily polluted rural North China Plain during the heating season. Science of the Total Environment, 2021, 789, 147956.	8.0	25
69	The decay of airborne bacteria and fungi in a constant temperature and humidity test chamber. Environment International, 2021, 157, 106816.	10.0	10
70	An unexpected large continental source of reactive bromine and chlorine with significant impact on wintertime air quality. National Science Review, 2021, 8, nwaa304.	9.5	42
71	Secondary Inorganic Ions Characteristics in PM _{2.5} Along Offshore and Coastal Areas of the Megacity Shanghai. Journal of Geophysical Research D: Atmospheres, 2021, 126, e2021JD035139.	3.3	9
72	Photochemical Aging of Atmospheric Fine Particles as a Potential Source for Gas-Phase Hydrogen Peroxide. Environmental Science & Technology, 2021, 55, 15063-15071.	10.0	8

#	Article	IF	CITATIONS
73	Winter ClNO ₂ formation in the region of fresh anthropogenic emissions: seasonal variability and insights into daytime peaks in northern China. Atmospheric Chemistry and Physics, 2021, 21, 15985-16000.	4.9	8
74	Overlooked Significant Impact of Trace Metals on the Bacterial Community of PM _{2.5} in High‶ime Resolution. Journal of Geophysical Research D: Atmospheres, 2021, 126, e2021JD035408.	3.3	3
75	Measurement report: Molecular characteristics of cloud water in southern China and insights into aqueous-phase processes from Fourier transform ion cyclotron resonance mass spectrometry. Atmospheric Chemistry and Physics, 2021, 21, 16631-16644.	4.9	11
76	Addressing Unresolved Complex Mixture of I/SVOCs Emitted From Incomplete Combustion of Solid Fuels by Nontarget Analysis. Journal of Geophysical Research D: Atmospheres, 2021, 126, e2021JD035835.	3.3	18
77	Satellite-based estimation of full-coverage ozone (O3) concentration and health effect assessment across Hainan Island. Journal of Cleaner Production, 2020, 244, 118773.	9.3	54
78	Separation and quantification of imidazoles in atmospheric particles using LC–Orbitrapâ€MS. Journal of Separation Science, 2020, 43, 577-589.	2.5	17
79	Different formation mechanisms of PAH during wood and coal combustion under different temperatures. Atmospheric Environment, 2020, 222, 117084.	4.1	48
80	Klarite as a label-free SERS-based assay: a promising approach for atmospheric bioaerosol detection. Analyst, The, 2020, 145, 277-285.	3.5	26
81	Enhanced aqueous-phase formation of secondary organic aerosols due to the regional biomass burning over North China Plain. Environmental Pollution, 2020, 256, 113401.	7.5	30
82	Satellite-Based Estimates of Wet Ammonium (NH ₄ -N) Deposition Fluxes Across China during 2011–2016 Using a Space–Time Ensemble Model. Environmental Science & Technology, 2020, 54, 13419-13428.	10.0	8
83	Preface. Journal of Environmental Sciences, 2020, 95, 1.	6.1	0
84	Inorganic composition and occult deposition of frost collected under severe polluted area in winter in the North China Plain. Science of the Total Environment, 2020, 722, 137911.	8.0	5
85	Production Flux and Chemical Characteristics of Spray Aerosol Generated From Raindrop Impact on Seawater and Soil. Journal of Geophysical Research D: Atmospheres, 2020, 125, e2019JD032052.	3.3	3
86	Effects of cleaner ship fuels on air quality and implications for future policy: A case study of Chongming Ecological Island in China. Journal of Cleaner Production, 2020, 267, 122088.	9.3	23
87	Photochemical Oxidation of Water-Soluble Organic Carbon (WSOC) on Mineral Dust and Enhanced Organic Ammonium Formation. Environmental Science & amp; Technology, 2020, 54, 15631-15642.	10.0	14
88	Daily CO2 Emission Reduction Indicates the Control of Activities to Contain COVID-19 in China. Innovation(China), 2020, 1, 100062.	9.1	25
89	Chemical Characteristics and Brown Carbon Chromophores of Atmospheric Organic Aerosols Over the Yangtze River Channel: A Cruise Campaign. Journal of Geophysical Research D: Atmospheres, 2020, 125, e2020JD032497.	3.3	16
90	Gaseous and Particulate Chlorine Emissions From Typical Iron and Steel Industry in China. Journal of Geophysical Research D: Atmospheres, 2020, 125, e2020JD032729.	3.3	13

#	Article	IF	CITATIONS
91	Water/Methanol-Insoluble Brown Carbon Can Dominate Aerosol-Enhanced Light Absorption in Port Cities. Environmental Science & Technology, 2020, 54, 14889-14898.	10.0	26
92	The pollution levels, variation characteristics, sources and implications of atmospheric carbonyls in a typical rural area of North China Plain during winter. Journal of Environmental Sciences, 2020, 95, 256-265.	6.1	15
93	Tris(2,4-di- <i>tert</i> -butylphenyl)phosphate: An Unexpected Abundant Toxic Pollutant Found in PM _{2.5} . Environmental Science & Technology, 2020, 54, 10570-10576.	10.0	39
94	Study of Secondary Organic Aerosol Formation from Chlorine Radical-Initiated Oxidation of Volatile Organic Compounds in a Polluted Atmosphere Using a 3D Chemical Transport Model. Environmental Science & Technology, 2020, 54, 13409-13418.	10.0	24
95	A More Important Role for the Ozoneâ€S(IV) Oxidation Pathway Due to Decreasing Acidity in Clouds. Journal of Geophysical Research D: Atmospheres, 2020, 125, e2020JD033220.	3.3	15
96	HONO Budget and Its Role in Nitrate Formation in the Rural North China Plain. Environmental Science & Technology, 2020, 54, 11048-11057.	10.0	74
97	Sizeâ€Resolved Mixing States and Sources of Amineâ€Containing Particles in the East China Sea. Journal of Geophysical Research D: Atmospheres, 2020, 125, e2020JD033162.	3.3	10
98	Detection of gaseous dimethylamine using vocus proton-transfer-reaction time-of-flight mass spectrometry. Atmospheric Environment, 2020, 243, 117875.	4.1	18
99	ROS-generation potential of Humic-like substances (HULIS) in ambient PM2.5 in urban Shanghai: Association with HULIS concentration and light absorbance. Chemosphere, 2020, 256, 127050.	8.2	26
100	Pollution levels, composition characteristics and sources of atmospheric PM2.5 in a rural area of the North China Plain during winter. Journal of Environmental Sciences, 2020, 95, 172-182.	6.1	22
101	Simultaneous determination of nine atmospheric amines and six inorganic ions by non-suppressed ion chromatography using acetonitrile and 18-crown-6 as eluent additive. Journal of Chromatography A, 2020, 1624, 461234.	3.7	11
102	Assessing the Effect of Reactive Oxygen Species and Volatile Organic Compound Profiles Coming from Certain Types of Chinese Cooking on the Toxicity of Human Bronchial Epithelial Cells. Environmental Science & Technology, 2020, 54, 8868-8877.	10.0	30
103	Marine organic matter in the remote environment of the Cape Verde islands – an introduction and overview to the MarParCloud campaign. Atmospheric Chemistry and Physics, 2020, 20, 6921-6951.	4.9	21
104	Nocturnal PM2.5 explosive growth dominates severe haze in the rural North China Plain. Atmospheric Research, 2020, 242, 105020.	4.1	20
105	Increasing surface ozone and enhanced secondary organic carbon formation at a city junction site: An epitome of the Yangtze River Delta, China (2014–2017). Environmental Pollution, 2020, 265, 114847.	7.5	16
106	The characteristics of atmospheric brown carbon in Xi'an, inland China: sources, size distributions and optical properties. Atmospheric Chemistry and Physics, 2020, 20, 2017-2030.	4.9	47
107	Forward ultra-low emission for power plants via wet electrostatic precipitators and newly developed demisters: Filterable and condensable particulate matters. Atmospheric Environment, 2020, 225, 117372.	4.1	36
108	Significant impact of coal combustion on VOCs emissions in winter in a North China rural site. Science of the Total Environment, 2020, 720, 137617.	8.0	63

#	Article	IF	CITATIONS
109	Online measurement of carbonaceous aerosols in suburban Shanghai during winter over a three-year period: Temporal variations, meteorological effects, and sources. Atmospheric Environment, 2020, 226, 117408.	4.1	24
110	Non-agricultural sources dominate the atmospheric NH3 in Xi'an, a megacity in the semi-arid region of China. Science of the Total Environment, 2020, 722, 137756.	8.0	50
111	Direct links between hygroscopicity and mixing state of ambient aerosols: estimating particle hygroscopicity from their single-particle mass spectra. Atmospheric Chemistry and Physics, 2020, 20, 6273-6290.	4.9	12
112	Sources and health risks of PM2.5-bound polychlorinated biphenyls (PCBs) and organochlorine pesticides (OCPs) in a North China rural area. Journal of Environmental Sciences, 2020, 95, 240-247.	6.1	17
113	Simulating the impacts of ship emissions on coastal air quality: Importance of a high-resolution emission inventory relative to cruise- and land-based observations. Science of the Total Environment, 2020, 728, 138454.	8.0	37
114	Complexation of Fe(III)/Catechols in atmospheric aqueous phase and the consequent cytotoxicity assessment in human bronchial epithelial cells (BEAS-2B). Ecotoxicology and Environmental Safety, 2020, 202, 110898.	6.0	10
115	Impact of quarantine measures on chemical compositions of PM2.5 during the COVID-19 epidemic in Shanghai, China. Science of the Total Environment, 2020, 743, 140758.	8.0	87
116	Size-resolved chemical composition analysis of ions produced by a commercial soft X-ray aerosol neutralizer. Journal of Aerosol Science, 2020, 147, 105586.	3.8	11
117	Atmospheric Photosensitization: A New Pathway for Sulfate Formation. Environmental Science & Technology, 2020, 54, 3114-3120.	10.0	65
118	Size-segregated characteristics of organic carbonÂ(OC), elemental carbonÂ(EC) and organic matter in particulate matterÂ(PM) emitted from different types of ships in China. Atmospheric Chemistry and Physics, 2020, 20, 1549-1564.	4.9	24
119	Nitrated phenols and the phenolic precursors in the atmosphere in urban Jinan, China. Science of the Total Environment, 2020, 714, 136760.	8.0	48
120	Effects of aerosol pollution on PM2.5-associated bacteria in typical inland and coastal cities of northern China during the winter heating season. Environmental Pollution, 2020, 262, 114188.	7.5	61
121	Estimation of Secondary Organic Aerosol Formation During a Photochemical Smog Episode in Shanghai, China. Journal of Geophysical Research D: Atmospheres, 2020, 125, e2019JD032033.	3.3	21
122	Molecular Characterization of Organosulfates in Highly Polluted Atmosphere Using Ultraâ€Highâ€Resolution Mass Spectrometry. Journal of Geophysical Research D: Atmospheres, 2020, 125, e2019JD032253.	3.3	18
123	Characterization of particulate matter and its extinction ability during different seasons and weather conditions in Sinkiang, China: two case studies. Environmental Science and Pollution Research, 2020, 27, 22414-22422.	5.3	2
124	The evolution of cloud and aerosol microphysics at the summit of Mt.ÂTai, China. Atmospheric Chemistry and Physics, 2020, 20, 13735-13751.	4.9	10
125	Nitrate-dominated PM _{2.5} and elevation of particle pH observed in urban Beijing during the winter of 2017. Atmospheric Chemistry and Physics, 2020, 20, 5019-5033.	4.9	70
126	Importance of gas-particle partitioning of ammonia in haze formation in the rural agricultural environment. Atmospheric Chemistry and Physics, 2020, 20, 7259-7269.	4.9	31

#	Article	IF	CITATIONS
127	Oxygenated products formed from OH-initiated reactions of trimethylbenzene: autoxidation and accretion. Atmospheric Chemistry and Physics, 2020, 20, 9563-9579.	4.9	29
128	Development of an automatic linear calibration method for high-resolution single-particle mass spectrometry: improved chemical species identification for atmospheric aerosols. Atmospheric Measurement Techniques, 2020, 13, 4111-4121.	3.1	6
129	Air pollution characteristics in China during 2015–2016: Spatiotemporal variations and key meteorological factors. Science of the Total Environment, 2019, 648, 902-915.	8.0	188
130	Unexpectedly Increased Particle Emissions from the Steel Industry Determined by Wet/Semidry/Dry Flue Gas Desulfurization Technologies. Environmental Science & Technology, 2019, 53, 10361-10370.	10.0	39
131	Dark air–liquid interfacial chemistry of glyoxal and hydrogen peroxide. Npj Climate and Atmospheric Science, 2019, 2, .	6.8	18
132	Chemistry-triggered events of PM2.5 explosive growth during late autumn and winter in Shanghai, China. Environmental Pollution, 2019, 254, 112864.	7.5	44
133	Evolution of aqSOA from the Air–Liquid Interfacial Photochemistry of Glyoxal and Hydroxyl Radicals. Environmental Science & Technology, 2019, 53, 10236-10245.	10.0	28
134	Enhanced heterogeneous uptake of sulfur dioxide on mineral particles through modification of iron speciation during simulated cloud processing. Atmospheric Chemistry and Physics, 2019, 19, 12569-12585.	4.9	18
135	Size-segregated water-soluble N-bearing species in the land-sea boundary zone of East China. Atmospheric Environment, 2019, 218, 116990.	4.1	2
136	Abundant NH ₃ in China Enhances Atmospheric HONO Production by Promoting the Heterogeneous Reaction of SO ₂ with NO ₂ . Environmental Science & Technology, 2019, 53, 14339-14347.	10.0	73
137	Pollutants emitted from typical Chinese vessels: Potential contributions to ozone and secondary organic aerosols. Journal of Cleaner Production, 2019, 238, 117862.	9.3	27
138	Sub-lethal concentrations of heavy metals induce antibiotic resistance via mutagenesis. Journal of Hazardous Materials, 2019, 369, 9-16.	12.4	89
139	The effect and mechanism of urban fine particulate matter (PM2.5) on horizontal transfer of plasmid-mediated antimicrobial resistance genes. Science of the Total Environment, 2019, 683, 116-123.	8.0	35
140	Characteristics of fine particle explosive growth events in Beijing, China: Seasonal variation, chemical evolution pattern and formation mechanism. Science of the Total Environment, 2019, 687, 1073-1086.	8.0	61
141	Excitation-emission matrix fluorescence, molecular characterization and compound-specific stable carbon isotopic composition of dissolved organic matter in cloud water over Mt. Tai. Atmospheric Environment, 2019, 213, 608-619.	4.1	25
142	Formation features of nitrous acid in the offshore area of the East China Sea. Science of the Total Environment, 2019, 682, 138-150.	8.0	25
143	Contribution of transregional transport to particle pollution and health effects in Shanghai during 2013–2017. Science of the Total Environment, 2019, 677, 564-570.	8.0	19
144	Impacts of six potential HONO sources on HOx budgets and SOA formation during a wintertime heavy haze period in the North China Plain. Science of the Total Environment, 2019, 681, 110-123.	8.0	40

#	Article	IF	CITATIONS
145	Inherent Metals of a Phytoremediation Plant Influence Its Recyclability by Hydrothermal Liquefaction. Environmental Science & Technology, 2019, 53, 6580-6586.	10.0	36
146	Size distribution and chemical composition of primary particles emitted during open biomass burning processes: Impacts on cloud condensation nuclei activation. Science of the Total Environment, 2019, 674, 179-188.	8.0	20
147	Size-fractionated water-soluble ions during autumn and winter: Insights into volatile ammonium formation mechanisms in Shanghai, a megacity of China. Atmospheric Environment: X, 2019, 2, 100011.	1.4	1
148	Cytotoxicity analysis of ambient fine particle in BEAS-2B cells on an air-liquid interface (ALI) microfluidics system. Science of the Total Environment, 2019, 677, 108-119.	8.0	13
149	Impact of emission controls on air quality in Beijing during APEC 2014: Implications from water-soluble ions and carbonaceous aerosol in PM2.5 and their precursors. Atmospheric Environment, 2019, 210, 241-252.	4.1	56
150	<i>In situ</i> remediation of subsurface contamination: opportunities and challenges for nanotechnology and advanced materials. Environmental Science: Nano, 2019, 6, 1283-1302.	4.3	65
151	The effects of firework regulation on air quality and public health during the Chinese Spring Festival from 2013 to 2017 in a Chinese megacity. Environment International, 2019, 126, 96-106.	10.0	64
152	Nitrogen-containing secondary organic aerosol formation by acrolein reaction with ammonia/ammonium. Atmospheric Chemistry and Physics, 2019, 19, 1343-1356.	4.9	21
153	Nitrite-Mediated Photooxidation of Vanillin in the Atmospheric Aqueous Phase. Environmental Science & Technology, 2019, 53, 14253-14263.	10.0	55
154	lsotopic constraints on the atmospheric sources and formation of nitrogenous species in clouds influenced by biomass burning. Atmospheric Chemistry and Physics, 2019, 19, 12221-12234.	4.9	19
155	The spatiotemporal variation and key factors of SO2 in 336 cities across China. Journal of Cleaner Production, 2019, 210, 602-611.	9.3	42
156	Emission factors and environmental implication of organic pollutants in PM emitted from various vessels in China. Atmospheric Environment, 2019, 200, 302-311.	4.1	40
157	A method for particulate matter 2.5 (PM2.5) biotoxicity assay using luminescent bacterium. Ecotoxicology and Environmental Safety, 2019, 170, 796-803.	6.0	9
158	Nonthermal air plasma dehydration of hydrochar improves its carbon sequestration potential and dissolved organic matter molecular characteristics. Science of the Total Environment, 2019, 659, 655-663.	8.0	23
159	Decarbonylation reaction of saturated and oxidized tar from pyrolysis of low aromaticity biomass boost reduction of hexavalent chromium. Chemical Engineering Journal, 2019, 360, 1042-1050.	12.7	14
160	Profile of inhalable bacteria in PM2.5 at Mt. Tai, China: Abundance, community, and influence of air mass trajectories. Ecotoxicology and Environmental Safety, 2019, 168, 110-119.	6.0	31
161	Photochemical Aging of Guaiacol by Fe(III)–Oxalate Complexes in Atmospheric Aqueous Phase. Environmental Science & Technology, 2019, 53, 127-136.	10.0	50
162	Impact of adsorbed nitrate on the heterogeneous conversion of SO2 on α-Fe2O3 in the absence and presence of simulated solar irradiation. Science of the Total Environment, 2019, 649, 1393-1402.	8.0	17

#	Article	IF	CITATIONS
163	Comparative Study of PAHs in PM1 and PM2.5 at a Background Site in the North China Plain. Aerosol and Air Quality Research, 2019, 19, 2281-2293.	2.1	10
164	Physiochemical characteristics of aerosol particles collected from the Jokhang Temple indoors and the implication to human exposure. Environmental Pollution, 2018, 236, 992-1003.	7.5	13
165	Baosteel emission control significantly benefited air quality in Shanghai. Journal of Environmental Sciences, 2018, 71, 127-135.	6.1	9
166	Petrol and diesel exhaust particles accelerate the horizontal transfer of plasmid-mediated antimicrobial resistance genes. Environment International, 2018, 114, 280-287.	10.0	44
167	Sub-inhibitory concentrations of heavy metals facilitate the horizontal transfer of plasmid-mediated antibiotic resistance genes in water environment. Environmental Pollution, 2018, 237, 74-82.	7.5	271
168	Trends in heterogeneous aqueous reaction in continuous haze episodes in suburban Shanghai: An in-depth case study. Science of the Total Environment, 2018, 634, 1192-1204.	8.0	32
169	Characterization and acid-mobilization study for typical iron-bearing clay mineral. Journal of Environmental Sciences, 2018, 71, 222-232.	6.1	15
170	Pollution characteristics of particulate matters emitted from outdoor barbecue cooking in urban Jinan in eastern China. Frontiers of Environmental Science and Engineering, 2018, 12, 1.	6.0	9
171	Influences of Temperature and Metal on Subcritical Hydrothermal Liquefaction of Hyperaccumulator: Implications for the Recycling of Hazardous Hyperaccumulators. Environmental Science & Technology, 2018, 52, 2225-2234.	10.0	61
172	Carbon transmission of CO ₂ activated nano-MgO carbon composites enhances phosphate immobilization. Journal of Materials Chemistry A, 2018, 6, 3705-3713.	10.3	37
173	A novel process for obtaining high quality cellulose acetate from green landscaping waste. Journal of Cleaner Production, 2018, 176, 338-347.	9.3	31
174	Nitro and oxy-PAHs bounded in PM2.5 and PM1.0 under different weather conditions at Mount Tai in Eastern China: Sources, long-distance transport, and cancer risk assessment. Science of the Total Environment, 2018, 622-623, 1400-1407.	8.0	14
175	Identification and semi-quantification of biogenic organic nitrates in ambient particulate matters by UHPLC/ESI-MS. Atmospheric Environment, 2018, 176, 140-147.	4.1	12
176	CO2 activation promotes available carbonate and phosphorus of antibiotic mycelial fermentation residue-derived biochar support for increased lead immobilization. Chemical Engineering Journal, 2018, 334, 1101-1107.	12.7	49
177	Optimizing xylose production from pinewood sawdust through dilute-phosphoric-acid hydrolysis by response surface methodology. Journal of Cleaner Production, 2018, 178, 572-579.	9.3	41
178	Key Role of Nitrate in Phase Transitions of Urban Particles: Implications of Important Reactive Surfaces for Secondary Aerosol Formation. Journal of Geophysical Research D: Atmospheres, 2018, 123, 1234-1243.	3.3	81
179	<scp>ToF IMS</scp> characterization of glyoxal surface oxidation products by hydrogen peroxide: A comparison between dry and liquid samples. Surface and Interface Analysis, 2018, 50, 927-938.	1.8	19
180	Investigation of new particle formation at the summit of Mt.ÂTai, China. Atmospheric Chemistry and Physics, 2018, 18, 2243-2258.	4.9	22

#	Article	IF	CITATIONS
181	An observational study of nitrous acid (HONO) in Shanghai, China: The aerosol impact on HONO formation during the haze episodes. Science of the Total Environment, 2018, 630, 1057-1070.	8.0	54
182	Associations between short-term exposure to ambient sulfur dioxide and increased cause-specific mortality in 272 Chinese cities. Environment International, 2018, 117, 33-39.	10.0	107
183	Observations of fine particulate nitrated phenols in four sites in northern China: concentrations, source apportionment, and secondary formation. Atmospheric Chemistry and Physics, 2018, 18, 4349-4359.	4.9	67
184	Pollutant emissions from residential combustion and reduction strategies estimated via a village-based emission inventory in Beijing. Environmental Pollution, 2018, 238, 230-237.	7.5	64
185	Characteristics of atmospheric ammonia and its relationship with vehicle emissions in a megacity in China. Atmospheric Environment, 2018, 182, 97-104.	4.1	36
186	Characteristics and sources of nitrous acid in an urban atmosphere of northern China: Results from 1-yr continuous observations. Atmospheric Environment, 2018, 182, 296-306.	4.1	82
187	Observations of atmospheric pollutants at Lhasa during 2014–2015: Pollution status and the influence of meteorological factors. Journal of Environmental Sciences, 2018, 63, 28-42.	6.1	31
188	Fog composition along the Yangtze River basin: Detecting emission sources of pollutants in fog water. Journal of Environmental Sciences, 2018, 71, 2-12.	6.1	15
189	Trash to treasure: Use flue gas SO2 to produce H2 via a photoelectrochemical process. Chemical Engineering Journal, 2018, 335, 231-235.	12.7	29
190	Activating Inert Alkaliâ€Metal Ions by Electron Transfer from Manganese Oxide for Formaldehyde Abatement. Chemistry - A European Journal, 2018, 24, 681-689.	3.3	29
191	Measurements of nonvolatile size distribution and its link to traffic soot in urban Shanghai. Science of the Total Environment, 2018, 615, 452-461.	8.0	2
192	Characteristics of the pollutant emissions in a tunnel of Shanghai on a weekday. Journal of Environmental Sciences, 2018, 71, 136-149.	6.1	11
193	Chromatographic separation of glucose, xylose and arabinose from lignocellulosic hydrolysates using cation exchange resin. Separation and Purification Technology, 2018, 195, 288-294.	7.9	28
194	Effect of relative humidity and the presence of aerosol particles on the α-pinene ozonolysis. Journal of Environmental Sciences, 2018, 71, 99-107.	6.1	10
195	Atmospheric PAHs, NPAHs, and OPAHs at an urban, mountainous, and marine sites in Northern China: Molecular composition, sources, and ageing. Atmospheric Environment, 2018, 173, 256-264.	4.1	64
196	Air quality in the middle and lower reaches of the Yangtze River channel: a cruise campaign. Atmospheric Chemistry and Physics, 2018, 18, 14445-14464.	4.9	9
197	Six sources mainly contributing to the haze episodes and health risk assessment of PM2.5 at Beijing suburb in winter 2016. Ecotoxicology and Environmental Safety, 2018, 166, 146-156.	6.0	51
198	Primary Particulate Matter Emitted from Heavy Fuel and Diesel Oil Combustion in a Typical Container Ship: Characteristics and Toxicity. Environmental Science & Technology, 2018, 52, 12943-12951.	10.0	69

#	Article	IF	CITATIONS
199	Cloud scavenging of anthropogenic refractory particles at a mountain site in North China. Atmospheric Chemistry and Physics, 2018, 18, 14681-14693.	4.9	25
200	Nano-metal oxides induce antimicrobial resistance via radical-mediated mutagenesis. Environment International, 2018, 121, 1162-1171.	10.0	55
201	Counteractive effects of regional transport and emission control on the formation of fine particles: a case study during the Hangzhou G20 summit. Atmospheric Chemistry and Physics, 2018, 18, 13581-13600.	4.9	43
202	Temporal variations in the hygroscopicity and mixing state of black carbon aerosols in a polluted megacity area. Atmospheric Chemistry and Physics, 2018, 18, 15201-15218.	4.9	24
203	Production Temperature Effects on the Structure of Hydrochar-Derived Dissolved Organic Matter and Associated Toxicity. Environmental Science & amp; Technology, 2018, 52, 7486-7495.	10.0	86
204	The changing ambient mixing ratios of long-lived halocarbons under Montreal Protocol in China. Journal of Cleaner Production, 2018, 188, 774-785.	9.3	19
205	Observation and analysis of atmospheric volatile organic compounds in a typical petrochemical area in Yangtze River Delta, China. Journal of Environmental Sciences, 2018, 71, 233-248.	6.1	66
206	Fine particulate matter constituents and stress hormones in the hypothalamus–pituitary–adrenal axis. Environment International, 2018, 119, 186-192.	10.0	84
207	Understanding unusually high levels of peroxyacetyl nitrate (PAN) in winter in Urban Jinan, China. Journal of Environmental Sciences, 2018, 71, 249-260.	6.1	38
208	Emerging investigator series: heterogeneous reactions of sulfur dioxide on mineral dust nanoparticles: from single component to mixed components. Environmental Science: Nano, 2018, 5, 1821-1833.	4.3	24
209	Molecular distributions of dicarboxylic acids, oxocarboxylic acids and <i>α</i> -dicarbonyls in PM _{2.5} collected at the top of Mt. Tai, North China, during the wheat burning season of 2014. Atmospheric Chemistry and Physics. 2018, 18, 10741-10758.	4.9	27
210	Characteristics and sources of atmospheric volatile organic compounds (VOCs) along the mid-lower Yangtze River in China. Atmospheric Environment, 2018, 190, 232-240.	4.1	50
211	Investigating particles, VOCs, ROS produced from mosquito-repellent incense emissions and implications in SOA formation and human health. Building and Environment, 2018, 143, 645-651.	6.9	22
212	Personal Ozone Exposure and Respiratory Inflammatory Response: The Role of DNA Methylation in the Arginase–Nitric Oxide Synthase Pathway. Environmental Science & Technology, 2018, 52, 8785-8791.	10.0	35
213	Atmospheric new particle formation from sulfuric acid and amines in a Chinese megacity. Science, 2018, 361, 278-281.	12.6	415
214	Does interfacial photochemistry play a role in the photolysis of pyruvic acid in water?. Atmospheric Environment, 2018, 191, 36-45.	4.1	28
215	Adsorption of SO2 on mineral dust particles influenced by atmospheric moisture. Atmospheric Environment, 2018, 191, 153-161.	4.1	26
216	The influence of temperature on the heterogeneous uptake of SO2 on hematite particles. Science of the Total Environment, 2018, 644, 1493-1502.	8.0	15

#	Article	IF	CITATIONS
217	Impact of heterogeneous uptake of nitrogen dioxide on the conversion of acetaldehyde on gamma-alumina in the absence and presence of simulated solar irradiation. Atmospheric Environment, 2018, 187, 282-291.	4.1	9
218	Diurnal concentrations, sources, and cancer risk assessments of PM2.5-bound PAHs, NPAHs, and OPAHs in urban, marine and mountain environments. Chemosphere, 2018, 209, 147-155.	8.2	40
219	Chemical Composition and Bacterial Community in Size-Resolved Cloud Water at the Summit of Mt. Tai, China. Aerosol and Air Quality Research, 2018, 18, 1-14.	2.1	13
220	Trend in Fine Sulfate Concentrations and the Associated Secondary Formation Processes at an Urban Site in North China. Aerosol and Air Quality Research, 2018, 18, 1519-1530.	2.1	4
221	Online single particle measurement of fireworks pollution during Chinese New Year in Nanning. Journal of Environmental Sciences, 2017, 53, 184-195.	6.1	41
222	Long-range and regional transported size-resolved atmospheric aerosols during summertime in urban Shanghai. Science of the Total Environment, 2017, 583, 334-343.	8.0	41
223	Physiochemical characteristics of aerosol particles in the typical microenvironment of hospital in Shanghai, China. Science of the Total Environment, 2017, 580, 651-659.	8.0	11
224	Investigation of diverse bacteria in cloud water at Mt. Tai, China. Science of the Total Environment, 2017, 580, 258-265.	8.0	37
225	Aerosol optical properties at urban and coastal sites in Shandong Province, Northern China. Atmospheric Research, 2017, 188, 39-47.	4.1	14
226	Ligand-Promoted Photoreductive Dissolution of Goethite by Atmospheric Low-Molecular Dicarboxylates. Journal of Physical Chemistry A, 2017, 121, 1647-1656.	2.5	29
227	Single Silver Adatoms on Nanostructured Manganese Oxide Surfaces: Boosting Oxygen Activation for Benzene Abatement. Environmental Science & amp; Technology, 2017, 51, 2304-2311.	10.0	106
228	Heterogeneous Nucleation of Trichloroethylene Ozonation Products in the Formation of New Fine Particles. Scientific Reports, 2017, 7, 42600.	3.3	4
229	Air pollution–aerosol interactions produce more bioavailable iron for ocean ecosystems. Science Advances, 2017, 3, e1601749.	10.3	182
230	Emission characterization, environmental impact, and control measure of PM2.5 emitted from agricultural crop residue burning in China. Journal of Cleaner Production, 2017, 149, 629-635.	9.3	107
231	Reaction Mechanism of 4-Chlorobiphenyl and the NO3Radical: An Experimental and Theoretical Study. Journal of Physical Chemistry A, 2017, 121, 3461-3468.	2.5	2
232	Surface-Enhanced Raman Spectroscopy: A Facile and Rapid Method for the Chemical Component Study of Individual Atmospheric Aerosol. Environmental Science & Technology, 2017, 51, 6260-6267.	10.0	68
233	Characterization of typical metal particles during haze episodes in Shanghai, China. Chemosphere, 2017, 181, 259-269.	8.2	20
234	Reconciling modeling with observations of radiative absorption of black carbon aerosols. Journal of Geophysical Research D: Atmospheres, 2017, 122, 5932-5942.	3.3	13

#	Article	IF	CITATIONS
235	Active Tetrahedral Iron Sites of γ-Fe ₂ O ₃ Catalyzing NO Reduction by NH ₃ . Environmental Science and Technology Letters, 2017, 4, 246-250.	8.7	47
236	Spatial and temporal variation of particulate matter and gaseous pollutants in China during 2014–2016. Atmospheric Environment, 2017, 161, 235-246.	4.1	131
237	Tuning electronic states of catalytic sites enhances SCR activity of hexagonal WO3by Mo framework substitution. Catalysis Science and Technology, 2017, 7, 2467-2473.	4.1	8
238	Enhanced Performance of Ceria-Based NO _{<i>x</i>} Reduction Catalysts by Optimal Support Effect. Environmental Science & Composition (2017, 51, 473-478.	10.0	77
239	Design and application of a novel integrated microsampling system for simultaneous collection of gas- and particle-phase semivolatile organic compounds. Atmospheric Environment, 2017, 149, 1-11.	4.1	7
240	Deciphering the aqueous chemistry of glyoxal oxidation with hydrogen peroxide using molecular imaging. Physical Chemistry Chemical Physics, 2017, 19, 20357-20366.	2.8	29
241	Carbonyl compounds at Mount Tai in the North China Plain: Characteristics, sources, and effects on ozone formation. Atmospheric Research, 2017, 196, 53-61.	4.1	48
242	Observations of N 2 O 5 and ClNO 2 at a polluted urban surface site in North China: High N 2 O 5 uptake coefficients and low ClNO 2 product yields. Atmospheric Environment, 2017, 156, 125-134.	4.1	90
243	Removal of SO ₂ on a nanoporous photoelectrode with simultaneous H ₂ production. Environmental Science: Nano, 2017, 4, 834-842.	4.3	30
244	Interfacial photochemistry of biogenic surfactants: a major source of abiotic volatile organic compounds. Faraday Discussions, 2017, 200, 59-74.	3.2	42
245	Bacterial characterization in ambient submicron particles during severe haze episodes at Ji'nan, China. Science of the Total Environment, 2017, 580, 188-196.	8.0	89
246	Clean production pathways for regional power-generation system under emission constraints: A case study of Shanghai, China. Journal of Cleaner Production, 2017, 143, 989-1000.	9.3	33
247	A review of biomass burning: Emissions and impacts on air quality, health and climate in China. Science of the Total Environment, 2017, 579, 1000-1034.	8.0	815
248	Subinhibitory Concentrations of Disinfectants Promote the Horizontal Transfer of Multidrug Resistance Genes within and across Genera. Environmental Science & Technology, 2017, 51, 570-580.	10.0	323
249	Light absorption enhancement of black carbon from urban haze in Northern China winter. Environmental Pollution, 2017, 221, 418-426.	7.5	61
250	Evaluation and potential improvements of WRF/CMAQ in simulating multi-levels air pollution in megacity Shanghai, China. Stochastic Environmental Research and Risk Assessment, 2017, 31, 2513-2526.	4.0	16
251	Seasonal contributions to size-resolved n-alkanes (C8–C40) in the Shanghai atmosphere from regional anthropogenic activities and terrestrial plant waxes. Science of the Total Environment, 2017, 579, 1918-1928.	8.0	31
252	Chemical composition, source, and process of urban aerosols during winter haze formation in Northeast China. Environmental Pollution, 2017, 231, 357-366.	7.5	89

#	Article	IF	CITATIONS
253	Effects of particulate matter from straw burning on lung fibrosis in mice. Environmental Toxicology and Pharmacology, 2017, 56, 249-258.	4.0	34
254	Chemical Characteristics of Organic Aerosols in Shanghai: A Study by Ultrahighâ€Performance Liquid Chromatography Coupled With Orbitrap Mass Spectrometry. Journal of Geophysical Research D: Atmospheres, 2017, 122, 11,703.	3.3	82
255	Characteristics of size-resolved atmospheric inorganic and carbonaceous aerosols in urban Shanghai. Atmospheric Environment, 2017, 167, 625-641.	4.1	37
256	Demethanation Trend of Hydrochar Induced by Organic Solvent Washing and Its Influence on Hydrochar Activation. Environmental Science & Technology, 2017, 51, 10756-10764.	10.0	42
257	Hydrothermal liquefaction of agricultural and forestry wastes: state-of-the-art review and future prospects. Bioresource Technology, 2017, 245, 1184-1193.	9.6	209
258	Uptake of Gaseous Alkylamides by Suspended Sulfuric Acid Particles: Formation of Ammonium/Aminium Salts. Environmental Science & Technology, 2017, 51, 11710-11717.	10.0	16
259	Top-down synthesis strategies: Maximum noble-metal atom efficiency in catalytic materials. Chinese Journal of Catalysis, 2017, 38, 1588-1596.	14.0	15
260	Atmospheric emissions of Cu and Zn from coal combustion in China: Spatio-temporal distribution, human health effects, and short-term prediction. Environmental Pollution, 2017, 229, 724-734.	7.5	28
261	Particulate Matter Exposure and Stress Hormone Levels. Circulation, 2017, 136, 618-627.	1.6	364
262	Preface on air quality in China. Science of the Total Environment, 2017, 603-604, 26.	8.0	4
263	Morphology, composition, and mixing state of primary particles from combustion sources — crop residue, wood, and solid waste. Scientific Reports, 2017, 7, 5047.	3.3	66
264	Fabrication, characterization, and stability of supported single-atom catalysts. Catalysis Science and Technology, 2017, 7, 4250-4258.	4.1	112
265	Chemical characterization and toxicity assessment of fine particulate matters emitted from the combustion of petrol and diesel fuels. Science of the Total Environment, 2017, 605-606, 172-179.	8.0	73
266	First results from light scattering enhancement factor over central Indian Himalayas during GVAX campaign. Science of the Total Environment, 2017, 605-606, 124-138.	8.0	13
267	Emissions of fine particulate nitrated phenols from the burning of five common types of biomass. Environmental Pollution, 2017, 230, 405-412.	7.5	73
268	Influence of fireworks displays on the chemical characteristics of PM2.5 in rural and suburban areas in Central and East China. Science of the Total Environment, 2017, 578, 476-484.	8.0	40
269	Formation, features and controlling strategies of severe haze-fog pollutions in China. Science of the Total Environment, 2017, 578, 121-138.	8.0	245
270	Chemical characteristics of PM1/PM2.5 and influence on visual range at the summit of Mount Tai, North China. Science of the Total Environment, 2017, 575, 458-466.	8.0	24

#	Article	IF	CITATIONS
271	Contributions and source identification of biogenic and anthropogenic hydrocarbons to secondary organic aerosols at Mt. Tai in 2014. Environmental Pollution, 2017, 220, 863-872.	7.5	49
272	lon exchange separation for recovery of monosaccharides, organic acids and phenolic compounds from hydrolysates of lignocellulosic biomass. Separation and Purification Technology, 2017, 172, 100-106.	7.9	41
273	Open burning of rice, corn and wheat straws: primary emissions, photochemical aging, and secondary organic aerosol formation. Atmospheric Chemistry and Physics, 2017, 17, 14821-14839.	4.9	66
274	Multi-pollutant emissions from the burning of major agricultural residues in China and the related health-economic effects. Atmospheric Chemistry and Physics, 2017, 17, 4957-4988.	4.9	50
275	Characteristics of bacterial community in cloud water at Mt Tai: similarity and disparity under polluted and non-polluted cloud episodes. Atmospheric Chemistry and Physics, 2017, 17, 5253-5270.	4.9	37
276	Fungi diversity in PM _{2. 5} and PM ₁ at the summit of Mt.ATai: abundance, size distribution, and seasonal variation. Atmospheric Chemistry and Physics, 2017, 17, 11247-11260.	4.9	24
277	Real-time aerosol optical properties, morphology and mixing states under clear, haze and fog episodes in the summer of urban Beijing. Atmospheric Chemistry and Physics, 2017, 17, 5079-5093.	4.9	23
278	Insight into winter haze formation mechanisms based on aerosol hygroscopicity and effective density measurements. Atmospheric Chemistry and Physics, 2017, 17, 7277-7290.	4.9	26
279	Size-resolved chemical composition, effective density, and optical properties of biomass burning particles. Atmospheric Chemistry and Physics, 2017, 17, 7481-7493.	4.9	36
280	Chemical composition and droplet size distribution of cloud at the summit of Mount Tai, China. Atmospheric Chemistry and Physics, 2017, 17, 9885-9896.	4.9	53
281	Direct observations of organic aerosols in common wintertime hazes in North China: insights into direct emissions from Chinese residential stoves. Atmospheric Chemistry and Physics, 2017, 17, 1259-1270.	4.9	56
282	Sodium Rivals Silver as Single-Atom Active Centers for Catalyzing Abatement of Formaldehyde. Environmental Science & Technology, 2017, 51, 7084-7090.	10.0	70
283	Mixed Chloride Aerosols and their Atmospheric Implications: A Review. Aerosol and Air Quality Research, 2017, 17, 878-887.	2.1	24
284	Influence of Cloud/Fog on Atmospheric VOCs in the Free Troposphere: A Case Study at Mount Tai in Eastern China. Aerosol and Air Quality Research, 2017, 17, 2401-2412.	2.1	13
285	Aromatic Hydrocarbons and Halocarbons at a Mountaintop in Southern China. Aerosol and Air Quality Research, 2016, 16, 478-491.	2.1	9
286	Size distribution of particle-associated polybrominated diphenyl ethers (PBDEs) and their implications for health. Atmospheric Measurement Techniques, 2016, 9, 1025-1037.	3.1	26
287	Reactions of Atmospheric Particulate Stabilized Criegee Intermediates Lead to High-Molecular-Weight Aerosol Components. Environmental Science & Technology, 2016, 50, 5702-5710.	10.0	54
288	Effect of glycerol as co-solvent on yields of bio-oil from rice straw through hydrothermal liquefaction. Bioresource Technology, 2016, 220, 471-478.	9.6	77

#	Article	IF	CITATIONS
289	Separation of highâ€purity syringol and acetosyringone from rice strawâ€derived bioâ€oil by combining the basificationâ€acidification process and column chromatography. Electrophoresis, 2016, 37, 2522-2530.	2.4	16
290	Intense secondary aerosol formation due to strong atmospheric photochemical reactions in summer: observations at a rural site in eastern Yangtze River Delta of China. Science of the Total Environment, 2016, 571, 1454-1466.	8.0	109
291	Insights into different nitrate formation mechanisms from seasonal variations of secondary inorganic aerosols in Shanghai. Atmospheric Environment, 2016, 145, 1-9.	4.1	50
292	Self-Protection Mechanism of Hexagonal WO ₃ –Based DeNO _{<i>x</i>} Catalysts against Alkali Poisoning. Environmental Science & Technology, 2016, 50, 11951-11956.	10.0	51
293	Effects of amines on particle growth observed in new particle formation events. Journal of Geophysical Research D: Atmospheres, 2016, 121, 324-335.	3.3	56
294	Catalytic hydrothermal liquefaction of rice straw in water/ethanol mixtures for high yields of monomeric phenols using reductive CuZnAl catalyst. Fuel Processing Technology, 2016, 154, 1-6.	7.2	35
295	Atmospheric outflow of PM2.5 saccharides from megacity Shanghai to East China Sea: Impact of biological and biomass burning sources. Atmospheric Environment, 2016, 143, 1-14.	4.1	73
296	Size distribution of particle-phase sugar and nitrophenol tracers during severe urban haze episodes in Shanghai. Atmospheric Environment, 2016, 145, 115-127.	4.1	73
297	Organosulfate Formation through the Heterogeneous Reaction of Sulfur Dioxide with Unsaturated Fatty Acids and Longâ€Chain Alkenes. Angewandte Chemie - International Edition, 2016, 55, 10336-10339.	13.8	63
298	The variation of characteristics of individual particles during the haze evolution in the urban Shanghai atmosphere. Atmospheric Research, 2016, 181, 95-105.	4.1	25
299	A conceptual framework for mixing structures in individual aerosol particles. Journal of Geophysical Research D: Atmospheres, 2016, 121, 13,784.	3.3	98
300	Synthesis, characterization and adsorption capacity of magnetic carbon composites activated by CO ₂ : implication for the catalytic mechanisms of iron salts. Journal of Materials Chemistry A, 2016, 4, 18942-18951.	10.3	33
301	Molecular characterization of atmospheric particulate organosulfates in three megacities at the middle and lower reaches of the Yangtze River. Atmospheric Chemistry and Physics, 2016, 16, 2285-2298.	4.9	89
302	Size distributions of polycyclic aromatic hydrocarbons in urban atmosphere: sorption mechanism and source contributions to respiratory deposition. Atmospheric Chemistry and Physics, 2016, 16, 2971-2983.	4.9	68
303	Significant increase of summertime ozone at Mount Tai in Central Eastern China. Atmospheric Chemistry and Physics, 2016, 16, 10637-10650.	4.9	192
304	Detection of atmospheric gaseous amines and amides by a high-resolution time-of-flight chemical ionization mass spectrometer with protonated ethanol reagent ions. Atmospheric Chemistry and Physics, 2016, 16, 14527-14543.	4.9	95
305	Formation of secondary aerosols from gasoline vehicle exhaust when mixing with SO ₂ . Atmospheric Chemistry and Physics, 2016, 16, 675-689.	4.9	70
306	Distribution and sources of air pollutants in the North China Plain based on on-road mobile measurements. Atmospheric Chemistry and Physics, 2016, 16, 12551-12565.	4.9	22

#	Article	IF	CITATIONS
307	Size distribution and mixing state of black carbon particles during a heavy air pollution episode in Shanghai. Atmospheric Chemistry and Physics, 2016, 16, 5399-5411.	4.9	82
308	Identification of concentrations and sources of PM2.5-bound PAHs in North China during haze episodes in 2013. Air Quality, Atmosphere and Health, 2016, 9, 823-833.	3.3	30
309	Characteristics of ambient volatile organic compounds and the influence of biomass burning at a rural site in Northern China during summer 2013. Atmospheric Environment, 2016, 124, 156-165.	4.1	54
310	Physiochemical properties of carbonaceous aerosol from agricultural residue burning: Density, volatility, and hygroscopicity. Atmospheric Environment, 2016, 140, 94-105.	4.1	41
311	Characteristics of carbonaceous aerosols: Impact of biomass burning and secondary formation in summertime in a rural area of the North China Plain. Science of the Total Environment, 2016, 557-558, 520-530.	8.0	46
312	Measurements of nitrous acid (HONO) in urban area of Shanghai, China. Environmental Science and Pollution Research, 2016, 23, 5818-5829.	5.3	25
313	Monophenols separation from monosaccharides and acids by two-stage nanofiltration and reverse osmosis in hydrothermal liquefaction hydrolysates. Journal of Membrane Science, 2016, 504, 141-152.	8.2	24
314	The active sites of supported silver particle catalysts in formaldehyde oxidation. Chemical Communications, 2016, 52, 9996-9999.	4.1	27
315	Online single particle analysis of chemical composition and mixing state of crop straw burning particles: from laboratory study to field measurement. Frontiers of Environmental Science and Engineering, 2016, 10, 244-252.	6.0	9
316	Chemical composition of PM2.5 and meteorological impact among three years in urban Shanghai, China. Journal of Cleaner Production, 2016, 112, 1302-1311.	9.3	109
317	Controllable synthesis of magnetic carbon composites with high porosity and strong acid resistance from hydrochar for efficient removal of organic pollutants: An overlooked influence. Carbon, 2016, 99, 338-347.	10.3	115
318	Improved performance of supported single-atom catalysts via increased surface active sites. Catalysis Communications, 2016, 75, 74-77.	3.3	26
319	Radiative absorption enhancement from coatings on black carbon aerosols. Science of the Total Environment, 2016, 551-552, 51-56.	8.0	86
320	Tracking the conversion of nitrogen during pyrolysis of antibiotic mycelial fermentation residues using XPS and TG-FTIR-MS technology. Environmental Pollution, 2016, 211, 20-27.	7.5	103
321	Bio-oil production from eight selected green landscaping wastes through hydrothermal liquefaction. RSC Advances, 2016, 6, 15260-15270.	3.6	37
322	Preventing smog crises in China and globally. Journal of Cleaner Production, 2016, 112, 1261-1271.	9.3	79
323	The effects of acetaldehyde, glyoxal and acetic acid on the heterogeneous reaction of nitrogen dioxide on gamma-alumina. Physical Chemistry Chemical Physics, 2016, 18, 9367-9376.	2.8	19
324	An estimation of CO 2 emission via agricultural crop residue open field burning in China from 1996 to 2013. Journal of Cleaner Production, 2016, 112, 2625-2631.	9.3	141

#	Article	IF	CITATIONS
325	A review of single aerosol particle studies in the atmosphere of East Asia: morphology, mixing state, source, and heterogeneous reactions. Journal of Cleaner Production, 2016, 112, 1330-1349.	9.3	235
326	Thermal desorption single particle mass spectrometry of ambient aerosol in Shanghai. Atmospheric Environment, 2015, 123, 407-414.	4.1	19
327	Highly Dense Isolated Metal Atom Catalytic Sites: Dynamic Formation and In Situ Observations. Chemistry - A European Journal, 2015, 21, 17397-17402.	3.3	36
328	Strong atmospheric new particle formation in winter in urban Shanghai, China. Atmospheric Chemistry and Physics, 2015, 15, 1769-1781.	4.9	147
329	Sea salt aerosols as a reactive surface for inorganic and organic acidic gases in the Arctic troposphere. Atmospheric Chemistry and Physics, 2015, 15, 11341-11353.	4.9	80
330	Mixing state and sources of submicron regional background aerosols in the northern Qinghai–Tibet Plateau and the influence of biomass burning. Atmospheric Chemistry and Physics, 2015, 15, 13365-13376.	4.9	32
331	Concentrations and solubility of trace elements in fine particles at a mountain site, southern China: regional sources and cloud processing. Atmospheric Chemistry and Physics, 2015, 15, 8987-9002.	4.9	68
332	Secondary organic aerosol formation from photochemical aging of light-duty gasoline vehicle exhausts in a smog chamber. Atmospheric Chemistry and Physics, 2015, 15, 9049-9062.	4.9	90
333	FORest Canopy Atmosphere Transfer (FORCAsT) 1.0: a 1-D model of biosphere–atmosphere chemical exchange. Geoscientific Model Development, 2015, 8, 3765-3784.	3.6	60
334	N-acetylcysteine attenuates cigaret smoke-induced pulmonary exacerbation in a mouse model of emphysema. Inhalation Toxicology, 2015, 27, 802-809.	1.6	4
335	Evolution of biomass burning smoke particles in the dark. Atmospheric Environment, 2015, 120, 244-252.	4.1	41
336	Theoretical study for OH radical-initiated atmospheric oxidation of ethyl acrylate. Chemosphere, 2015, 119, 626-633.	8.2	25
337	Identification of the typical metal particles among haze, fog, and clear episodes in the Beijing atmosphere. Science of the Total Environment, 2015, 511, 369-380.	8.0	69
338	Separation of phenolic compounds with modified adsorption resin from aqueous phase products of hydrothermal liquefaction of rice straw. Bioresource Technology, 2015, 182, 160-168.	9.6	56
339	Enhanced formation of fine particulate nitrate at a rural site on the North China Plain in summer: The important roles of ammonia and ozone. Atmospheric Environment, 2015, 101, 294-302.	4.1	121
340	Do vehicular emissions dominate the source of C6–C8 aromatics in the megacity Shanghai of eastern China?. Journal of Environmental Sciences, 2015, 27, 290-297.	6.1	18
341	Rate coefficients for the reaction of ozone with 2- and 3-carene. Chemical Physics Letters, 2015, 621, 71-77.	2.6	12
342	Seasonal variation and difference of aerosol optical properties in columnar and surface atmospheres over Shanghai. Atmospheric Environment, 2015, 123, 315-326.	4.1	76

#	Article	IF	CITATIONS
343	Photosensitized Production of Atmospherically Reactive Organic Compounds at the Air/Aqueous Interface. Journal of the American Chemical Society, 2015, 137, 8348-8351.	13.7	97
344	Combustion of hazardous biological waste derived from the fermentation of antibiotics using TG–FTIR and Py–GC/MS techniques. Bioresource Technology, 2015, 193, 156-163.	9.6	104
345	Individual particle analysis of aerosols collected at Lhasa City in the Tibetan Plateau. Journal of Environmental Sciences, 2015, 29, 165-177.	6.1	38
346	The mechanism and kinetic model on the OH-initiated degradation of acetofenate in the atmosphere. Atmospheric Environment, 2015, 103, 357-364.	4.1	5
347	Investigation on the Physical and Chemical Properties of Hydrochar and Its Derived Pyrolysis Char for Their Potential Application: Influence of Hydrothermal Carbonization Conditions. Energy & Fuels, 2015, 29, 5222-5230.	5.1	56
348	Modification in light absorption cross section of laboratory-generated black carbon-brown carbon particles upon surface reaction and hydration. Atmospheric Environment, 2015, 116, 253-261.	4.1	16
349	Environmental performances of hydrochar-derived magnetic carbon composite affected by its carbonaceous precursor. RSC Advances, 2015, 5, 60713-60722.	3.6	38
350	Atmospheric degradation of lindane and 1,3-dichloroacetone in the gas phase. Studies at the EUPHORE simulation chamber. Chemosphere, 2015, 138, 112-119.	8.2	17
351	Levels, indoor–outdoor relationships and exposure risks of airborne particle-associated perchlorate and chlorate in two urban areas in Eastern Asia. Chemosphere, 2015, 135, 31-37.	8.2	19
352	Interactions between Heterogeneous Uptake and Adsorption of Sulfur Dioxide and Acetaldehyde on Hematite. Journal of Physical Chemistry A, 2015, 119, 4001-4008.	2.5	35
353	Two-stage nanofiltration process for high-value chemical production from hydrolysates of lignocellulosic biomass through hydrothermal liquefaction. Separation and Purification Technology, 2015, 147, 276-283.	7.9	33
354	Role of Hydrochar Properties on the Porosity of Hydrochar-based Porous Carbon for Their Sustainable Application. ACS Sustainable Chemistry and Engineering, 2015, 3, 833-840.	6.7	109
355	Macroalgae for biofuels production: Progress and perspectives. Renewable and Sustainable Energy Reviews, 2015, 47, 427-437.	16.4	280
356	Atmospheric Chemistry of Oxygenated Volatile Organic Compounds: Impacts on Air Quality and Climate. Chemical Reviews, 2015, 115, 3984-4014.	47.7	374
357	Effect of Formaldehyde on the Heterogeneous Reaction of Nitrogen Dioxide on Î ³ -Alumina. Journal of Physical Chemistry A, 2015, 119, 9317-9324.	2.5	14
358	HONO and its potential source particulate nitrite at an urban site in North China during the cold season. Science of the Total Environment, 2015, 538, 93-101.	8.0	59
359	PM2.5 pollution episode and its contributors from 2011 to 2013 in urban Shanghai, China. Atmospheric Environment, 2015, 123, 298-305.	4.1	46
360	Alkali- and Sulfur-Resistant Tungsten-Based Catalysts for NO _{<i>x</i>} Emissions Control. Environmental Science & Technology, 2015, 49, 14460-14465.	10.0	76

#	Article	IF	CITATIONS
361	Mechanistic and kinetic studies on OH-initiated atmospheric oxidation degradation of benzo[î±]pyrene in the presence of O2 and NOx. Chemosphere, 2015, 119, 387-393.	8.2	29
362	Size-resolved effective density of urban aerosols in Shanghai. Atmospheric Environment, 2015, 100, 133-140.	4.1	52
363	Spectral Light Absorption of Ambient Aerosols in Urban Beijing during Summer: An Intercomparison of Measurements from a Range of Instruments. Aerosol and Air Quality Research, 2015, 15, 1178-1187.	2.1	18
364	Design and characterization of a smog chamber for studying gas-phase chemical mechanisms and aerosol formation. Atmospheric Measurement Techniques, 2014, 7, 301-313.	3.1	89
365	Selective Extraction of Bio-oil from Hydrothermal Liquefaction of Salix psammophila by Organic Solvents with Different Polarities through Multistep Extraction Separation. BioResources, 2014, 9, .	1.0	51
366	Using hourly measurements to explore the role of secondary inorganic aerosol in PM2.5 during haze and fog in Hangzhou, China. Advances in Atmospheric Sciences, 2014, 31, 1427-1434.	4.3	52
367	Magnetic activated carbon prepared from rice straw-derived hydrochar for triclosan removal. RSC Advances, 2014, 4, 63620-63626.	3.6	75
368	The Impact of Nonlocal Ammonia on Submicron Particulate Matter and Visibility Degradation in Urban Shanghai. Advances in Meteorology, 2014, 2014, 1-12.	1.6	8
369	Characterization of aerosol optical properties, chemical composition and mixing states in the winter season in Shanghai, China. Journal of Environmental Sciences, 2014, 26, 2412-2422.	6.1	9
370	Fog Formation in Cold Season in Ji'nan, China: Case Analyses with Application of HYSPLIT Model. Advances in Meteorology, 2014, 2014, 1-8.	1.6	5
371	Hygroscopicity and optical properties of alkylaminium sulfates. Journal of Environmental Sciences, 2014, 26, 37-43.	6.1	9
372	Novel and High-Performance Magnetic Carbon Composite Prepared from Waste Hydrochar for Dye Removal. ACS Sustainable Chemistry and Engineering, 2014, 2, 969-977.	6.7	131
373	Preparation of magnetic porous carbon from waste hydrochar by simultaneous activation and magnetization for tetracycline removal. Bioresource Technology, 2014, 154, 209-214.	9.6	341
374	Reaction pathway for reactivation and aging of paraoxon-inhibited-acetylcholinesterase: A QM/MM study. Computational and Theoretical Chemistry, 2014, 1035, 44-50.	2.5	8
375	Airborne submicron particulate (PM1) pollution in Shanghai, China: Chemical variability, formation/dissociation of associated semi-volatile components and the impacts on visibility. Science of the Total Environment, 2014, 473-474, 199-206.	8.0	84
376	Characteristics and chemical compositions of particulate matter collected at the selected metro stations of Shanghai, China. Science of the Total Environment, 2014, 496, 443-452.	8.0	64
377	Analysis of human breath samples of lung cancer patients and healthy controls with solid-phase microextraction (SPME) and flow-modulated comprehensive two-dimensional gas chromatography (GC × GC). Analytical Methods, 2014, 6, 6841.	2.7	44
378	Indoor PM2.5 and its chemical composition during a heavy haze–fog episode at Jinan, China. Atmospheric Environment, 2014, 99, 641-649.	4.1	38

#	Article	IF	CITATIONS
379	Role of Water Molecule in the Gas-Phase Formation Process of Nitrated Polycyclic Aromatic Hydrocarbons in the Atmosphere: A Computational Study. Environmental Science & Technology, 2014, 48, 5051-5057.	10.0	93
380	Particle number concentration, size distribution and chemical composition during haze and photochemical smog episodes in Shanghai. Journal of Environmental Sciences, 2014, 26, 1894-1902.	6.1	57
381	Observations of linear dependence between sulfate and nitrate in atmospheric particles. Journal of Geophysical Research D: Atmospheres, 2014, 119, 341-361.	3.3	45
382	Online hygroscopicity and chemical measurement of urban aerosol in Shanghai, China. Atmospheric Environment, 2014, 95, 318-326.	4.1	33
383	Facile Fabrication of Magnetic Carbon Composites from Hydrochar via Simultaneous Activation and Magnetization for Triclosan Adsorption. Environmental Science & Technology, 2014, 48, 5840-5848.	10.0	144
384	Computational Evidence for the Detoxifying Mechanism of Epsilon Class Glutathione Transferase Toward the Insecticide DDT. Environmental Science & Technology, 2014, 48, 5008-5016.	10.0	47
385	Severe haze episodes and seriously polluted fog water in Ji'nan, China. Science of the Total Environment, 2014, 493, 133-137.	8.0	71
386	Characteristics and relevant remote sources of black carbon aerosol in Shanghai. Atmospheric Research, 2014, 135-136, 159-171.	4.1	38
387	Fractional iron solubility of aerosol particles enhanced by biomass burning and ship emission in Shanghai, East China. Science of the Total Environment, 2014, 481, 377-391.	8.0	38
388	Mechanistic and kinetic studies on the OH-initiated atmospheric oxidation of fluoranthene. Science of the Total Environment, 2014, 490, 639-646.	8.0	23
389	Composition and hygroscopicity of aerosol particles at Mt. Lu in South China: Implications for acid precipitation. Atmospheric Environment, 2014, 94, 626-636.	4.1	30
390	A novel porous carbon derived from hydrothermal carbon for efficient adsorption of tetracycline. Carbon, 2014, 77, 627-636.	10.3	249
391	Impacts of new particle formation on aerosol cloud condensation nuclei (CCN) activity in Shanghai: case study. Atmospheric Chemistry and Physics, 2014, 14, 11353-11365.	4.9	34
392	Variations of cloud condensation nuclei (CCN) and aerosol activity during fog–haze episode: a case study from Shanghai. Atmospheric Chemistry and Physics, 2014, 14, 12499-12512.	4.9	38
393	A study of aerosol liquid water content based on hygroscopicity measurements at high relative humidity in the North China Plain. Atmospheric Chemistry and Physics, 2014, 14, 6417-6426.	4.9	131
394	Aerosol hygroscopicity parameter derived from the light scattering enhancement factor measurements in the North China Plain. Atmospheric Chemistry and Physics, 2014, 14, 8105-8118.	4.9	84
395	The effects of nitrate on the heterogeneous uptake of sulfur dioxide on hematite. Atmospheric Chemistry and Physics, 2014, 14, 9451-9467.	4.9	61
396	Size distribution of water-soluble inorganic ions in urban aerosols in Shanghai. Atmospheric Pollution Research, 2014, 5, 639-647.	3.8	31

#	Article	IF	CITATIONS
397	Mixing state and hygroscopicity of dust and haze particles before leaving Asian continent. Journal of Geophysical Research D: Atmospheres, 2014, 119, 1044-1059.	3.3	67
398	Size Distribution and Optical Properties of Ambient Aerosols during Autumn in Orleans, France. Aerosol and Air Quality Research, 2014, 14, 744-755.	2.1	2
399	Hydrothermal Liquefaction of Water Hyacinth: Product Distribution and Identification. Energy Sources, Part A: Recovery, Utilization and Environmental Effects, 2013, 35, 1349-1357.	2.3	21
400	Hygroscopic growth of urban aerosol particles during the 2009 Mirage-Shanghai Campaign. Atmospheric Environment, 2013, 64, 263-269.	4.1	61
401	Measurements of surface cloud condensation nuclei and aerosol activity in downtown Shanghai. Atmospheric Environment, 2013, 69, 354-361.	4.1	35
402	Consecutive transport of anthropogenic air masses and dust storm plume: Two case events at Shanghai, China. Atmospheric Research, 2013, 127, 22-33.	4.1	51
403	Aerosol single scattering albedo affected by chemical composition: An investigation using CRDS combined with MARGA. Atmospheric Research, 2013, 124, 149-157.	4.1	27
404	Determination of organic pollutants in coking wastewater by dispersive liquid-liquid microextraction/GC/MS. Journal of Separation Science, 2013, 36, 1644-1651.	2.5	21
405	Microscopic Evaluation of Trace Metals in Cloud Droplets in an Acid Precipitation Region. Environmental Science & Technology, 2013, 47, 4172-4180.	10.0	59
406	Reaction of NO ₂ with Selected Conjugated Alkenes. Journal of Physical Chemistry A, 2013, 117, 14132-14140.	2.5	9
407	Megacity impacts on regional ozone formation: observations and WRF-Chem modeling for the MIRACE-Shanghai field campaign. Atmospheric Chemistry and Physics, 2013, 13, 5655-5669.	4.9	132
408	Effects of Ammonia and Amines on Heterogeneous Oxidation of Carbonyl Sulfide on Hematite. Wuli Huaxue Xuebao/ Acta Physico - Chimica Sinica, 2013, 29, 2027-2034.	4.9	3
409	A case study of the highly time-resolved evolution of aerosol chemical and optical properties in urban Shanghai, China. Atmospheric Chemistry and Physics, 2013, 13, 3931-3944.	4.9	56
410	Hydrothermal Liquefaction of Desert Shrub Salix psammophila to High Value-added Chemicals and Hydrochar with Recycled Processing Water. BioResources, 2013, 8, .	1.0	43
411	Urban Aerosol Characteristics during the World Expo 2010 in Shanghai. Aerosol and Air Quality Research, 2013, 13, 36-48.	2.1	16
412	Agricultural Fires and Their Potential Impacts on Regional Air Quality over China. Aerosol and Air Quality Research, 2013, 13, 992-1001.	2.1	49
413	Single particle analysis of amines in ambient aerosol in Shanghai. Environmental Chemistry, 2012, 9, 202.	1.5	54
414	A parameterization of low visibilities for hazy days in the North China Plain. Atmospheric Chemistry and Physics, 2012, 12, 4935-4950.	4.9	138

#	Article	IF	CITATIONS
415	Morphology, composition and mixing state of individual carbonaceous aerosol in urban Shanghai. Atmospheric Chemistry and Physics, 2012, 12, 693-707.	4.9	96
416	A simplified electrospray ionization source based on electrostatic field induction for mass spectrometric analysis of droplet samples. Analyst, The, 2012, 137, 5743.	3.5	9
417	Solubility of Iron from Combustion Source Particles in Acidic Media Linked to Iron Speciation. Environmental Science & Technology, 2012, 46, 11119-11127.	10.0	80
418	Evolution of the mixing state of fine aerosols during haze events in Shanghai. Atmospheric Research, 2012, 104-105, 193-201.	4.1	74
419	Measurements of surface aerosol optical properties in winter of Shanghai. Atmospheric Research, 2012, 109-110, 25-35.	4.1	65
420	Diurnal variations of organic molecular tracers and stable carbon isotopic composition in atmospheric aerosols over Mt. Tai in the North China Plain: an influence of biomass burning. Atmospheric Chemistry and Physics, 2012, 12, 8359-8375.	4.9	141
421	Conducting polymers in environmental analysis. TrAC - Trends in Analytical Chemistry, 2012, 39, 163-179.	11.4	105
422	Liquefaction of Macroalgae Enteromorpha prolifera in Sub-/Supercritical Alcohols: Direct Production of Ester Compounds. Energy & Fuels, 2012, 26, 2342-2351.	5.1	108
423	Source and deposition of polycyclic aromatic hydrocarbons to Shanghai, China. Journal of Environmental Sciences, 2012, 24, 116-123.	6.1	26
424	Rush-hour aromatic and chlorinated hydrocarbons in selected subway stations of Shanghai, China. Journal of Environmental Sciences, 2012, 24, 131-141.	6.1	19
425	CFD modeling of a UV-LED photocatalytic odor abatement process in a continuous reactor. Journal of Hazardous Materials, 2012, 215-216, 25-31.	12.4	57
426	Columnar Optical Depth and Vertical Distribution of Aerosols over Shanghai. Aerosol and Air Quality Research, 2012, 12, 320-330.	2.1	8
427	Aerosol Size Spectra and Particle Formation Events at Urban Shanghai in Eastern China. Aerosol and Air Quality Research, 2012, 12, 1362-1372.	2.1	40
428	Characterization of polycyclic aromatic hydrocarbons in fog–rain events. Journal of Environmental Monitoring, 2011, 13, 2988.	2.1	35
429	Particle Size Distribution and Polycyclic Aromatic Hydrocarbons Emissions from Agricultural Crop Residue Burning. Environmental Science & Technology, 2011, 45, 5477-5482.	10.0	202
430	Dimethyl Sulfide Photocatalytic Degradation in a Light-Emitting-Diode Continuous Reactor: Kinetic and Mechanistic Study. Industrial & Engineering Chemistry Research, 2011, 50, 7977-7984.	3.7	60
431	Size-resolved hygroscopicity of submicrometer urban aerosols in Shanghai during wintertime. Atmospheric Research, 2011, 99, 353-364.	4.1	49
432	Monitoring optical properties of aerosols with cavity ringâ€down spectroscopy. Journal of Aerosol Science, 2011, 42, 277-284.	3.8	31

#	Article	IF	CITATIONS
433	Size-resolved and bulk activation properties of aerosols in the North China Plain. Atmospheric Chemistry and Physics, 2011, 11, 3835-3846.	4.9	110
434	An Improved Oddy Test Using Metal Films. Studies in Conservation, 2011, 56, 138-153.	1.1	11
435	Potential particulate pollution derived from UV-induced degradation of odorous dimethyl sulfide. Journal of Environmental Sciences, 2011, 23, 51-59.	6.1	14
436	Hygroscopicity and evaporation of ammonium chloride and ammonium nitrate: Relative humidity and size effects on the growth factor. Atmospheric Environment, 2011, 45, 2349-2355.	4.1	88
437	Fog water chemistry in Shanghai. Atmospheric Environment, 2011, 45, 4034-4041.	4.1	61
438	Insights into summertime haze pollution events over Shanghai based on online water-soluble ionic composition of aerosols. Atmospheric Environment, 2011, 45, 5131-5137.	4.1	221
439	Hygroscopicity of ambient submicron particles in urban Hangzhou, China. Frontiers of Environmental Science and Engineering in China, 2011, 5, 342-347.	0.8	12
440	Important role of ammonia on haze formation in Shanghai. Environmental Research Letters, 2011, 6, 024019.	5.2	99
441	Effects of Nitrates on the Heterogeneous Reaction of Carbonyl Sulfide on Model Aerosols. Wuli Huaxue Xuebao/ Acta Physico - Chimica Sinica, 2011, 27, 2275-2281.	4.9	0
442	Molecular characterization of urban organic aerosol in tropical India: contributions of primary emissions and secondary photooxidation. Atmospheric Chemistry and Physics, 2010, 10, 2663-2689.	4.9	200
443	Real-time, single-particle measurements of ambient aerosols in Shanghai. Frontiers of Chemistry in China: Selected Publications From Chinese Universities, 2010, 5, 331-341.	0.4	2
444	Physical characterization of aerosol particles during the Chinese New Year's firework events. Atmospheric Environment, 2010, 44, 5191-5198.	4.1	102
445	Synchronous role of coupled adsorption and photocatalytic oxidation on ordered mesoporous anatase TiO2–SiO2 nanocomposites generating excellent degradation activity of RhB dye. Applied Catalysis B: Environmental, 2010, 95, 197-207.	20.2	152
446	Insights into Ammonium Particle-to-Gas Conversion: Non-sulfate Ammonium Coupling with Nitrate and Chloride. Aerosol and Air Quality Research, 2010, 10, 589-595.	2.1	61
447	Chemical characterization of aerosols over the Atlantic Ocean and the Pacific Ocean during two cruises in 2007 and 2008. Journal of Geophysical Research, 2010, 115, .	3.3	25
448	Evidence for High Molecular Weight Nitrogen-Containing Organic Salts in Urban Aerosols. Environmental Science & Technology, 2010, 44, 4441-4446.	10.0	99
449	Hydrothermal Liquefaction of Macroalgae Enteromorpha prolifera to Bio-oil. Energy & Fuels, 2010, 24, 4054-4061.	5.1	474
450	Agricultural Fire Impacts on the Air Quality of Shanghai during Summer Harvesttime. Aerosol and Air Quality Research, 2010, 10, 95-101.	2.1	60

#	Article	IF	CITATIONS
451	Hygroscopicity of Inorganic Aerosols: Size and Relative Humidity Effects on the Growth Factor. Aerosol and Air Quality Research, 2010, 10, 255-264.	2.1	89
452	Synthesis of small crystal zeolite beta in a biphasic H2O–CTAB–alcohol system. Materials Letters, 2009, 63, 343-345.	2.6	15
453	Continuous measurement of peroxyacetyl nitrate (PAN) in suburban and remote areas of western China. Atmospheric Environment, 2009, 43, 228-237.	4.1	86
454	Direct quantification of organic acids in aerosols by desorption electrospray ionization mass spectrometry. Atmospheric Environment, 2009, 43, 2717-2720.	4.1	28
455	Single particle mass spectrometry of oxalic acid in ambient aerosols in Shanghai: Mixing state and formation mechanism. Atmospheric Environment, 2009, 43, 3876-3882.	4.1	103
456	Laboratory simulation of SO2 heterogeneous reactions on hematite surface under different SO2 concentrations. Journal of Environmental Sciences, 2009, 21, 1103-1107.	6.1	5
457	Determination of Alkyl Polycyclic Aromatic Hydrocarbons in Dustfall by Supercritical Fluid Extraction Followed by Gas Chromatography/Mass Spectrum. Bulletin of Environmental Contamination and Toxicology, 2009, 82, 189-193.	2.7	12
458	A multifunctional HTDMA system with a robust temperature control. Advances in Atmospheric Sciences, 2009, 26, 1235-1240.	4.3	18
459	Direct quantification of PAHs in biomass burning aerosols by desorption electrospray ionization mass spectrometry. International Journal of Mass Spectrometry, 2009, 281, 31-36.	1.5	27
460	Particulate Nitrate Formation in a Highly Polluted Urban Area: A Case Study by Single-Particle Mass Spectrometry in Shanghai. Environmental Science & Technology, 2009, 43, 3061-3066.	10.0	101
461	Source apportionment of lead-containing aerosol particles in Shanghai using single particle mass spectrometry. Chemosphere, 2009, 74, 501-507.	8.2	132
462	Photoinduced Formation of Fe(III)â^'Sulfato Complexes on the Surface of α-Fe ₂ O ₃ and Their Photochemical Performance. Journal of Physical Chemistry C, 2009, 113, 11316-11322.	3.1	17
463	Distribution and source of alkyl polycyclic aromatic hydrocarbons in dustfall in Shanghai, China: the effect on the coastal area. Journal of Environmental Monitoring, 2009, 11, 187-192.	2.1	26
464	Electrodeposited polyaniline as a fiber coating for solidâ€phase microextraction of organochlorine pesticides from water. Journal of Separation Science, 2008, 31, 2839-2845.	2.5	50
465	Synthesis and Structural Studies of 1â€Đeoxybaccatin VI Derivatives. Chinese Journal of Chemistry, 2008, 26, 1870-1878.	4.9	4
466	Rapid analysis of svoc in aerosols by desorption electrospray ionization mass spectrometry. Journal of the American Society for Mass Spectrometry, 2008, 19, 450-454.	2.8	26
467	Characteristics of trace elements and lead isotope ratios in PM2.5 from four sites in Shanghai. Journal of Hazardous Materials, 2008, 156, 36-43.	12.4	134
468	Flavonoid triglycosides from the seeds of Camellia oleifera Abel. Chinese Chemical Letters, 2008, 19, 1315-1318.	9.0	18

#	Article	IF	CITATIONS
469	Polythiophene as a novel fiber coating for solid-phase microextraction. Journal of Chromatography A, 2008, 1198-1199, 7-13.	3.7	54
470	A laboratory study of agricultural crop residue combustion in China: Emission factors and emission inventory. Atmospheric Environment, 2008, 42, 8432-8441.	4.1	202
471	Photocatalytic Degradation of RhB by Fluorinated Bi ₂ WO ₆ and Distributions of the Intermediate Products. Environmental Science & Technology, 2008, 42, 2085-2091.	10.0	351
472	Mesoporous bismuth titanate with visible-light photocatalytic activity. Chemical Communications, 2008, , 4977.	4.1	51
473	The Influences of Heterogeneous Reaction on Particle Optical Properties: A Laboratory Case of SO2 on Hematite and Hematite-NaCl Mixture. , 2008, , .		0
474	Modeling secondary organic aerosol formation through cloud processing of organic compounds. Atmospheric Chemistry and Physics, 2007, 7, 5343-5355.	4.9	71
475	Climatology of aerosol radiative properties in northern China. Atmospheric Research, 2007, 84, 132-141.	4.1	10
476	Controllable and Repeatable Synthesis of Thermally Stable Anatase Nanocrystalâ^'Silica Composites with Highly Ordered Hexagonal Mesostructures. Journal of the American Chemical Society, 2007, 129, 13894-13904.	13.7	233
477	Heterogeneous Uptake of Carbonyl Sulfide on Hematite and Hematiteâ^'NaCl Mixtures. Environmental Science & Technology, 2007, 41, 6484-6490.	10.0	30
478	Heterogeneous Uptake and Oxidation of SO2 on Iron Oxides. Journal of Physical Chemistry C, 2007, 111, 6077-6085.	3.1	202
479	Benz[a]anthracene Heterogeneous Photochemical Reaction on the Surface of TiO2 Particles. Acta Physico-chimica Sinica, 2007, 23, 1531-1536.	0.6	11
480	Heterogeneous Chemistry of Organic Acids on Soot Surfaces. Journal of Physical Chemistry A, 2007, 111, 4804-4814.	2.5	26
481	Analysis of chloro- and nitrobenzenes in water by a simple polyaniline-based solid-phase microextraction coupled with gas chromatography. Journal of Chromatography A, 2007, 1140, 21-28.	3.7	56
482	Diastereomers of Dibromo-7-epi-10-deacetylcephalomannine:  Crowded and Cytotoxic Taxanes Exhibit Halogen Bonds. Journal of Medicinal Chemistry, 2006, 49, 1891-1899.	6.4	73
483	Heterogeneous Reactions of Sulfur Dioxide on Typical Mineral Particles. Journal of Physical Chemistry B, 2006, 110, 12588-12596.	2.6	129
484	Conversion of taxane glycosides to 10-deacetylbaccatin III. Natural Product Research, 2006, 20, 119-124.	1.8	7
485	Heterogeneous Reactions of Methylglyoxal in Acidic Media:Â Implications for Secondary Organic Aerosol Formation. Environmental Science & Technology, 2006, 40, 7682-7687.	10.0	175
486	Heterogeneous photocatalytic decomposition of benzene on lanthanum-doped TiO2 film at ambient temperature. Chemosphere, 2006, 65, 2282-2288.	8.2	45

#	Article	IF	CITATIONS
487	Synthesis and crystal structure of 7,9-dideacetyl-1-deoxybaccatinVI. Journal of Chemical Crystallography, 2006, 36, 337-341.	1.1	9
488	Distribution and Source of Polycyclic Aromatic Hydrocarbons (PAHs) on Dust Collected in Shanghai, People's Republic of China. Bulletin of Environmental Contamination and Toxicology, 2006, 76, 442-449.	2.7	19
489	The ion chemistry, seasonal cycle, and sources of PM2.5 and TSP aerosol in Shanghai. Atmospheric Environment, 2006, 40, 2935-2952.	4.1	463
490	A comparison of dust properties between China continent and Korea, Japan in East Asia. Atmospheric Environment, 2006, 40, 5787-5797.	4.1	54
491	Polycyclic aromatic hydrocarbons in dust from computers: one possible indoor source of human exposure. Atmospheric Environment, 2006, 40, 6956-6965.	4.1	47
492	Determination of PAHS in Dust from Shanghai by Optimized SFE and GC/MS. Annali Di Chimica, 2006, 96, 669-680.	0.6	7
493	Synthesis and Antitumor Activity of 20-O-Linked Succinate-Based Camptothecin Ester Derivatives. Letters in Drug Design and Discovery, 2006, 3, 83-86.	0.7	7
494	Synthesis and crystal structure of 2-debenzoyl and 4-deacetyl 1-deoxybaccatin VI derivatives. Journal of Molecular Structure, 2005, 738, 59-65.	3.6	10
495	A lead isotope record of shanghai atmospheric lead emissions in total suspended particles during the period of phasing out of leaded gasoline. Atmospheric Environment, 2005, 39, 1245-1253.	4.1	251
496	Crystallographic determination of stereochemistry of biologically active 2″,3″-dibromo-7-epi-10-deacetylcephalomannine. Bioorganic and Medicinal Chemistry Letters, 2005, 15, 839-842.	2.2	9
497	Photooxidation of carbonyl sulfide in the presence of the typical oxides in atmospheric aerosol. Science in China Series B: Chemistry, 2005, 48, 31-37.	0.8	10
498	Speciation of the elements and compositions on the surfaces of dust storm particles: The evidence for the coupling of iron with sulfur in aerosol during the long-range trans-port. Science Bulletin, 2005, 50, 738.	1.7	0
499	Preparation and evaluation of new brominated paclitaxel analogues. Journal of Asian Natural Products Research, 2005, 7, 231-236.	1.4	0
500	Photooxidation of carbonyl sulfide in the presence of the typical oxides in atmospheric aerosol. Science in China Series B: Chemistry, 2005, 48, 31.	0.8	1
501	Mechanism of the heteroge-neous reaction of carbonyl sulfide with typical compo-nents of atmospheric aerosol. Science Bulletin, 2004, 49, 1231.	1.7	10
502	Carbonyl Sulfide Derived from Catalytic Oxidation of Carbon Disulfide over Atmospheric Particles. Environmental Science & Technology, 2001, 35, 2543-2547.	10.0	29
503	Catalytic oxidation of CS2 over atmospheric particles and oxide catalysts. Science in China Series B: Chemistry, 2001, 44, 587-595.	0.8	5
504	A Large Scale Separation of Taxanes from the Bark Extract of <i>Taxus yunnanesis</i> and ¹ Hâ€and ¹³ Câ€NMR Assignments for 7 <i>â€epiâ€</i> 10â€Deacetyltaxol. Chinese Jou Chemistry, 2001, 19, 82-90.	urrana∳of	9

#	Article	IF	CITATIONS
505	LARGE-SCALE PROCESS FOR HIGH PURITY TAXOL FROM BARK EXTRACT OF TAXUS YUNNANESIS. Journal of Liquid Chromatography and Related Technologies, 2000, 23, 2499-2512.	1.0	4
506	Temperature-programmed desorption of pyridine on solid superacids. Materials Chemistry and Physics, 1996, 45, 220-222.	4.0	5
507	Studies on SO 4 2? promoted mixed oxide superacids. Catalysis Letters, 1996, 37, 187-191.	2.6	49
508	Electroanalytical studies of chlorophylls and their determination. Electroanalysis, 1991, 3, 827-831.	2.9	0
509	Mechanism of poisoning of the V2O5/TiO2 catalyst for the reduction of NO by NH3. Journal of Catalysis, 1990, 125, 411-420.	6.2	214
510	Transesterification of Jatropha Oil to Biodiesel by Using Catalyst Containing Ca(C ₃ H ₇ O ₃) ₂ as a Solid Base Catalyst. Advanced Materials Research, 0, 666, 93-102.	0.3	3